Ceramics International 47 (2021) 29504–29508

Contents lists available at ScienceDirect

Ceramics International

journal homepage: www.elsevier.com/locate/ceramint

Influence of microstructure and magnetizing mechanisms on magnetic complex permeability (imaginary part) of a Cu-doped Ni–Zn polycrystalline ferrite

A. Barba-Juan [a,b], N. Vicente [a,b], A. Mormeneo-Segarra [a,b], C. Clausell-Terol [a,b,*]

[a] Departamento de Ingeniería Química, Universitat Jaume I, 12071, Castellón, Spain
[b] Instituto Universitario de Tecnología Cerámica, Universitat Jaume I, 12071, Castellón, Spain

ARTICLE INFO

Keywords:
Ni-Zn ferrites
Complex magnetic permeability
Microstructure
Magnetizing mechanism
Spin rotation
Domain-wall motion

ABSTRACT

The complex permeability of the Cu-doped Ni–Zn polycrystalline ferrites is strongly dependent on microstructure, particularly on relative density (ϕ) and average grain size (G), as it has been shown in a previous study developed at a constant angular frequency (10^7 Hz). In this study, the previous microstructural model proposed has been extended to an angular frequency range (from 10^6 to 10^9 Hz) demonstrating its validity and reliability. In addition, domain-wall motion and spin rotation contributions to magnetic permeability have been individually considered in the mathematical model, highlighting the relative influence of each magnetizing mechanism at different angular frequencies.

1. Introduction

One of the main applications of ferrites is in the elimination of electromagnetic wave pollution due to their electromagnetic interferences (EMI) shielding properties. Among the ferrites used in this field, two types stand out: NiZn and MnZn ferrites. The most widely used are NiZn ones, generally doped with copper, since their angular frequency range is in the higher frequency region (>10 MHz), whereas in the case of MnZn ferrites it is limited to a few MHz [1,2].

The magnetic properties of these materials are mainly determined by their chemical composition and final microstructure (i.e. average grain size and relative density) [3]. The ferrite powder can be processed to obtain two types of bulk materials: ferrite *composite* materials, where particles are embedded in a polymeric matrix, and *sintered* ferrites, where particles are processed following the traditional ceramic route [4].

Magnetic permeability μ is a complex property when an alternating current (AC) magnetic field of angular frequency ω is applied to the material. Therefore, materials can be characterized by its complex permeability (real part and imaginary part) vs angular frequency spectrum, which is usually known in literature as the frequency dispersion of the material [5]. In polycrystalline ferrites, the frequency dispersion of complex permeability shows several characteristic magnetic resonances [6–9].

Literature highlights two kind of magnetizing mechanisms, spin rotation and domain-wall motion, both contributing to the real (μ') and imaginary part (μ'') of magnetic permeability [10]. In small grains (below $\sim$ 6 μm), where no magnetic domain-walls can be found at intragranular level, only monodomain state exists. In this case, magnetic permeability cannot be explained by domain-wall phenomena and only spin rotation exists. As the grain size increases (up to $\sim$ 25 μm) both domain-wall and spin rotation determine magnetic permeability [11,12].

Accordingly, a magnetic susceptibility for domain-wall motion (χ'_{DW} and χ''_{DW}) and a magnetic susceptibility for a spin rotation (χ'_S and χ''_S) can be defined and related to magnetic permeability as follows [3]:

$$\mu'(\omega) = 1 + \chi'_S(\omega) + \chi'_{DW}(\omega) \quad (1)$$

$$\mu''(\omega) = \chi''_S(\omega) + \chi''_{DW}(\omega) \quad (2)$$

In polycrystalline ferrites is usually observed that the higher the frequency of the magnetic field, the lower the influence of the domain-wall mechanism [7–10].

On the other hand, although magnetic properties of polycrystalline ferrites are extremely dependent on the microstructure of the sintered bodies, only spare information is found on mathematical relationship

* Corresponding author. Departamento de Ingeniería Química, Universitat Jaume I, 12071, Castellón, Spain.
E-mail address: cclausel@uji.es (C. Clausell-Terol).

https://doi.org/10.1016/j.ceramint.2021.07.119
Received 28 March 2021; Received in revised form 1 July 2021; Accepted 13 July 2021
Available online 14 July 2021

between microstructure and magnetic permeability [3,13–17].

In a previous paper [3], a new model linking effective (experimental) magnetic permeability (imaginary μ''_{eff}) or susceptibility (imaginary χ''_{eff}) to microstructure, based on Pankert equation [17] was proposed. The resulting equation includes average grain size (G), densification (ψ), domain-wall width (d_W) and permeability (imaginary μ''_i) of the bulk material:

$$\mu''_{eff}(\omega) = \mu''_i(\omega) \cdot \frac{G^2}{4 \cdot \pi^2 \cdot d_W^2 + G^2} \cdot \psi \tag{3}$$

where densification (an effective concept when comparing systems of different initial porosities [18]) can be calculated from the real (ρ_{real}) and theoretical densities ($\rho_{theoretical}$):

$$\psi = \frac{\frac{\rho_{real}}{\rho_{theoretical}} - \frac{\rho_{lim}}{\rho_{theoretical}}}{\frac{\rho_{theoretical}}{\rho_{theoretical}} - \frac{\rho_{lim}}{\rho_{theoretical}}} = \frac{\phi - \phi_{lim}}{1 - \phi_{lim}} \tag{4}$$

and where ϕ_{lim} represents the relative density below which the value of the magnetic permeability is close to zero. This experimental value can be estimated by plotting relative density (ϕ) vs magnetic permeability (μ''_{eff}) and extrapolating to $\mu''_{eff} = 0$. This limiting relative density depends not only on the sintering conditions but also on the green microstructure, which is mainly set by the particle size distribution of the raw materials and the shaping conditions.

Equation (3) was successfully tested and validated at a frequency of 10^7 Hz in the aforementioned previous study [3]. However, equation (3) does not contain the spin rotation and domain-wall motion contribution to the effective magnetic permeability of polycrystalline ferrites.

The aim of this paper is twofold. First, to validate equation (3) in the angular frequency range from 10^6 to 10^9 Hz, which corresponds to the working area of the Cu-doped Ni–Zn-polycrystalline ferrites used as EMI shielding and suppression materials. Second, to establish the contribution of the spin rotation and domain-wall motion magnetizing mechanisms to the effective magnetic permeability.

2. Experimental procedure

Ferrite powder of composition $Cu_{0,12}Ni_{0,23}Zn_{0,65}(Fe_2O_4)$ provided by *Fair-Rite Products Coorp* (Wallkill, EEUU) was used as raw material. While characteristics and physical properties of this industrial powder can be found in aforementioned previous paper [3], brief description of experimental procedure is given here. Powder was shaped by uniaxial pressing at six different pressures and sintered at eight temperatures and different dwell times, leading into 594 different final microstructures covering a wide range of relative density and average grain size values. A detailed description of the experimental procedure is given in previous papers [19,20].

True density of ferrite was 5380 kg/m^3 (experimentally determined on a helium pycnometer). Bulk density of each specimen was determined by the Archimedes method and relative density (ϕ) was calculated as the quotient of bulk density to true density. Average grain size was determined from grain size distribution using an image analysis of the cross-sectional area of the rectangular thermal etched surface of each specimen using scanning electron microscopy (SEM).

Complex magnetic permeability (real μ'_{eff} and imaginary μ''_{eff} parts) was measured on an Agilent E4991A RF impedance/material analyser in a frequency range of 1–1000 MHz using an Agilent 16454 A magnetic material test fixture.

3. Results and discussion

The microstructural properties and complex magnetic permeability (imaginary μ''_{eff}) of the sintered Cu-doped Ni–Zn-polycrystalline ferrite for the different pressing conditions can be found in the Supplementary Tables 1 to 6. The sintered microstructure of the specimens has been characterized by their average grain size G and relative density ϕ. Fig. 1 shows the frequency dispersion spectra of the imaginary part of the complex magnetic permeability (imaginary μ''_{eff}) of two sintered specimens with very different microstructures ($G = 3,45\ \mu m$; $\phi = 0,87$ and $G = 23,15\ \mu m$; $\phi = 0,96$). As may be observed in this figure, microstructure has a remarkable influence on the values of μ''_{eff} particularly at the angular frequencies of 10^6 and 10^7 Hz.

As it has been previously demonstrated [3], μ''_{eff} increases with relative density (ϕ) and, particularly, with average grain size (G) up to a limiting value of around 20–25 μm, from which properties worsen significantly due to the presence of trapped pores within grains and precipitated non-magnetic phases on grain boundaries [4,21–27]. Therefore, data of grains with size larger than the limiting value abovementioned have been removed and discussion has been focussed only on the 464 remaining experimental points.

Figs. 2 and 3 depict the distribution of μ''_{eff} vs average grain size for all the 464 analysed specimens at the four angular frequencies tested: 10^6, 10^7, 10^8 and 10^9 Hz. Trendline is similar for the four cases and can be divided in three sections: blue ($\phi < 0,80$), red ($0,80 \leq \phi < 0,90$), and green ($0,90 \leq \phi < 0,96$), reflecting the influence of relative density on μ''_{eff}. It may be observed that for low angular frequencies (10^6 and 10^7 Hz) the experimental data tend to a high value of μ''_{eff} (around 1400 and 550, respectively), whereas for high angular frequencies tend to a low value of μ''_{eff}: around 70 for 10^8 Hz and close to zero for 10^9 Hz. This experimental evidence can be explained by the different magnetizing mechanisms acting on the magnetic permeability (spin rotation and domain-wall), and by the fact that the contribution of domain-wall mechanism decreases as angular frequency raises [7,9]. Consequently, polycrystalline ferrite microstructure plays an important role on the magnetic permeability only at the angular frequencies in which both mechanisms are operating (10^6 and 10^7 Hz). At 10^8 Hz the influence of microstructure is minimal, and at 10^9 Hz microstructure has no influence at all on the magnetic permeability, which is indeed only governed by the spin rotation mechanism.

The sharp and drastic decline of μ''_{eff} when angular frequency increases at 10^8 Hz and, specially, at 10^9 Hz (observed in Figs. 1–3) explains why the Ni–Zn ferrite works as EMI suppressor in the frequency range 10^6–10^8 Hz, showing an absorption maximum around 10^7 Hz, as it has been previously stated by the authors (Clausell-Terol et al., submitted).

Previously, authors [3] had proposed equation (3), showing that it is a useful mathematical relationship between μ''_{eff} and microstructural

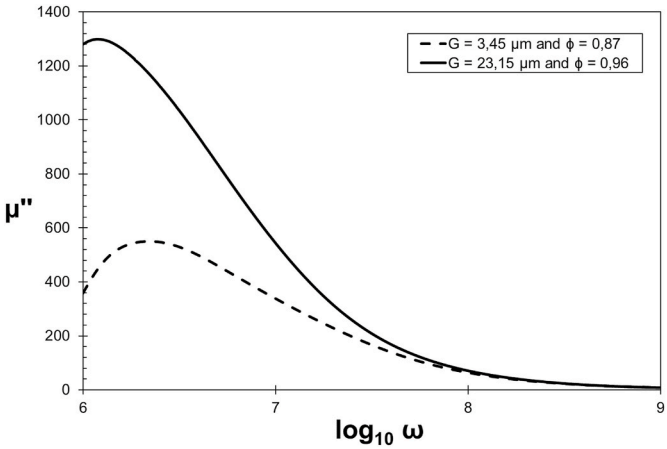

Fig. 1. Frequency dispersion spectra of the imaginary part of the complex magnetic permeability (μ''_{eff}) of two specimens with very different microstructures.

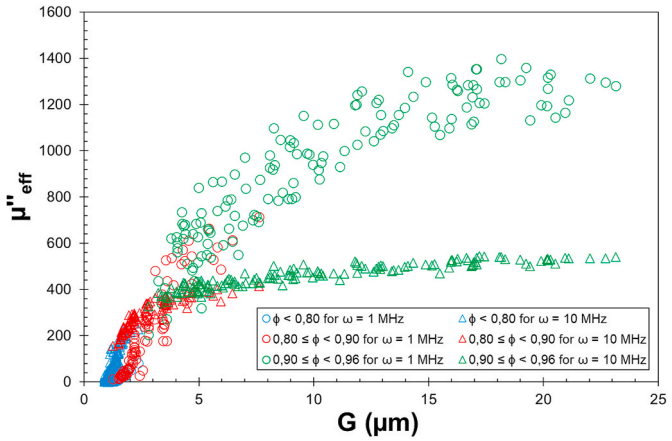

Fig. 2. Experimental results of μ''_{eff} vs average grain size at 10^6 and 10^7 Hz.

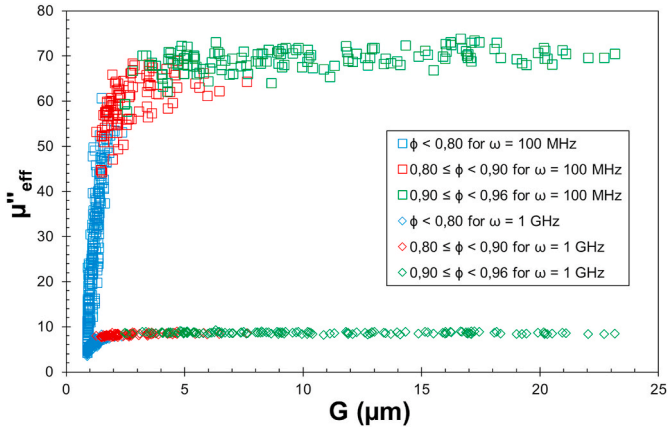

Fig. 3. Experimental results of μ''_{eff} vs average grain size at 10^8 and 10^9 Hz.

parameters, which accurately reproduces the experimental data for the angular frequency of 10^7 Hz. However, when equation (3) is used to reproduce experimental data for the angular frequencies tested in this paper (10^6, 10^8 and 10^9 Hz), no coherent results are obtained. In order to find a mathematical relationship valid for the full angular frequency range, equation (3) has been modified, including both contributions to the magnetic permeability (spin rotation - μ''_S and domain-wall - μ''_{DW}), as follows:

$$\mu''_{eff}(\omega) = \mu''_S(\omega)\cdot\psi + \mu''_{DW}(\omega)\cdot\left(\frac{G^2}{b'' + G^2}\right)\cdot\psi \tag{5}$$

where:

$$b'' = 4\cdot\pi^2\cdot {d_w}^2 \tag{6}$$

Equation (5) reveals that domain-wall contribution to magnetic permeability is strongly dependent on average grain size G and relative density ϕ, whereas spin rotation contribution depends on relative density ϕ but not on average grain size G [7]. In equation (5) μ''_S, μ''_{DW}, and b'' are fitting parameters to the experimental data. A nonlinear least-squares method has been used to fit data to equation (5), allowing the determination of constants μ''_S, μ''_{DW}, and b'' by minimizing the sum of squared residuals, for each tested angular frequency value.

Previously to this nonlinear fitting, ϕ_{lim} must be estimated to calculate ψ according to equation (4) for all experimental data. As an example, Fig. 4 depicts the relative density ϕ dependence on μ''_{eff} for the angular frequency of 10^6 Hz (the rest of angular frequencies lead to similar plots). This plot allows determining an estimated value of ϕ_{lim}

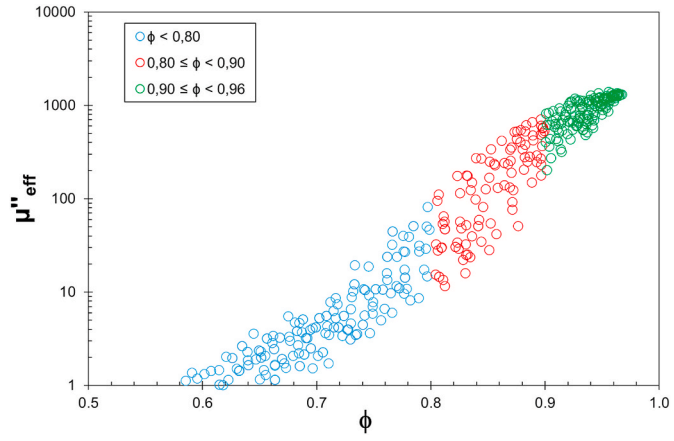

Fig. 4. Experimental results of μ''_{eff} vs relative density at 10^6 Hz for estimating the ϕ_{lim}.

around 0,65, which is slightly different from the previously used in Ref. [3] (ϕ_{lim} around 0,56) but is a more realistic value. In this case, the dispersion of μ''_{eff} experimental values when they tend to zero (see Fig. 4) has been taken into account, as well as for the rest of tested angular frequencies. Thus, 0,65 is the lowest relative density (ϕ_{lim}) value below which the value of the magnetic permeability μ''_{eff} becomes virtually zero. In fact, the experimental points corresponding to a very low value of relative density (ϕ) and average grain size (G) in Figs. 2 and 3 correspond to those specimens with an effective complex magnetic permeability-imaginary part value close to zero (see the Supplementary Tables 1 to 6).

Table 1 details the estimated values of constants μ''_S, μ''_{DW}, and b''. In order to use these values in equation (5) to reproduce experimental data, an empirical relationship between relative density (ϕ) and average grain size (G) must be obtained. To display this, the evolution of ϕ with G has been plotted in Fig. 5, given a nonlinear fit of the following empirical equation:

$$\phi = 0,915\cdot\left(\frac{G^{1,833}}{0,408 + G^{1,819}}\right) \tag{7}$$

Therefore, considering the previously obtained μ''_S, μ''_{DW}, and b'' constants (Table 1), the empirical equation (7) and the established value of ϕ_{lim}, equation (5) can be rewritten as follows:

$$\mu''_{eff}(\omega) = \left[\mu''_S(\omega) + \mu''_{DW}(\omega)\cdot\left(\frac{G^2}{b'' + G^2}\right)\right]\cdot\frac{0,915\cdot\left(\frac{G^{1,833}}{0,408+G^{1,819}}\right) - 0,65}{1 - 0,65} \tag{8}$$

which may be expected to satisfactorily reproduce the experimental data. In effect, Fig. 6 shows the calculated μ''_{eff} values using equation (8) (continuous line), along with the experimental data (discrete points), for the angular frequencies of 10^6, 10^7 and 10^8 Hz. Results corresponding to the angular frequency of 10^9 Hz are not included in Fig. 6 because, in this case, the μ''_{eff} values are very close to zero. As it can be observed, the mathematical model accurately reproduces the experimental data to any

Table 1
Values of the parameters estimated from equations (5) and (6).

Parameter	Angular frequency, ω (Hz)			
	10^6	10^7	10^8	10^9
μ''_S	25	50	45	11,5
μ''_{DW}	1500	550	35	0
b''	26,5	1,5	0,16	0
d_W (nm)	819	195	64	0

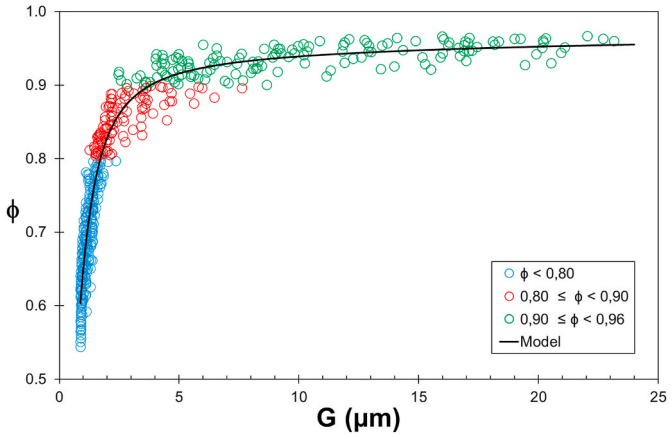

Fig. 5. Relative density vs average grain size.

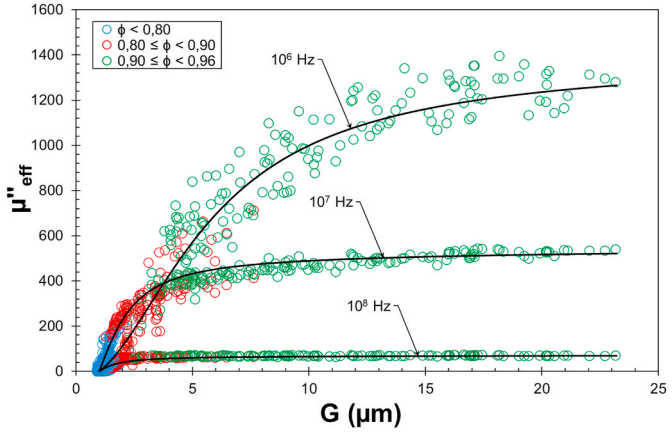

Fig. 6. Experimental and calculated values of μ''_{eff} using equation (8) at 10^6, 10^7 and 10^8 Hz.

angular frequency. Given the simplicity of the proposed equation and the possible sources of error in determining microstructural parameters, the agreement between theoretical and experimental data is very satisfactory.

Fig. 7 depicts the μ''_S and μ''_{DW} values shown in Table 1 versus angular frequency, allowing the following conclusions to be drawn:

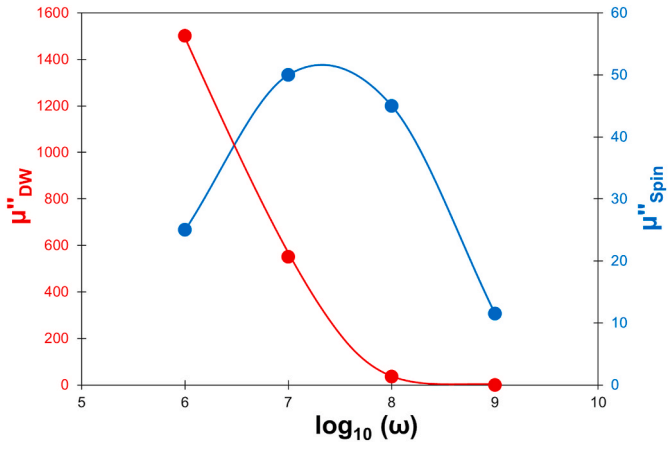

Fig. 7. Contribution of spin rotation and domain-wall magnetic mechanisms to the complex magnetic permeability – imaginary part at the four tested angular frequencies.

i) at low angular frequencies (10^6 and 10^7 Hz) the contribution of domain-wall to the complex magnetic permeability - imaginary part is more important than spin rotation contribution, whereas at high angular frequencies (10^8 and 10^9 Hz) contributions of both mechanisms are in the same order of magnitude;

ii) μ''_S presents a maximum value around 10^7 Hz, while μ''_{DW} sharply decreases with the rise in angular frequency; behaviours that are consistent with the ferrite complex permeability spectra found in literature [2,5,7–10,21,28–30];

iii) the higher values of μ''_{DW} observed at 10^6 and 10^7 Hz yield high complex magnetic permeability - imaginary part values in the studied ferrite, which makes it a very interesting material as EMI suppressor at these angular frequencies, although it does not present technological interest at higher angular frequencies (10^8 and 10^9 Hz).

Table 1 also details the calculated values of b'' and d_w using equation (6). The domain-wall width (d_w) drops sharply with the rise of angular frequency and becomes zero for the 10^9 Hz highest angular frequency (see Fig. 8). The domain-wall width concept was introduced by Pankert [15] as a natural length scale substantiating the grain size dependence of magnetic permeability. He also postulated its dependence on magnetic susceptibility and, hence, on angular frequency (as it has been observed in this study). The value of d_W at 10^7 Hz is consistent (virtually the same, ≈ 200 nm) with the value previously reported [3].

Comparison of Fig. 7 with Fig. 8 shows that the lower domain-wall width, the lower contribution of domain-wall motion mechanism to the magnetic permeability.

4. Conclusions

The effective complex magnetic permeability – imaginary part μ''_{eff} of a Cu-doped Ni–Zn polycrystalline ferrite used as EMI suppressor has been quantitatively related to microstructural parameters of the specimens (i.e., average grain size G and relative density ϕ). In this work an equation has been developed to extend the mathematical model validity of a previous published equation [3] relating μ''_{eff} to G and ϕ to a broader range of angular frequencies (between 10^6 and 10^9 Hz). Modified equation considers both spin rotation (μ''_S) and domain-wall (μ''_{DW}) contribution to the complex magnetic permeability – imaginary part and postulates that domain-wall contribution to magnetic permeability is strongly dependent on average grain size (G) and relative density (ϕ), whereas spin rotation contribution depends on relative density (ϕ) but not on average grain size (G). This new model allows to accurately reproduce the experimental values of μ''_{eff} to any angular frequency, as long as the average grain size and relative density of specimens are

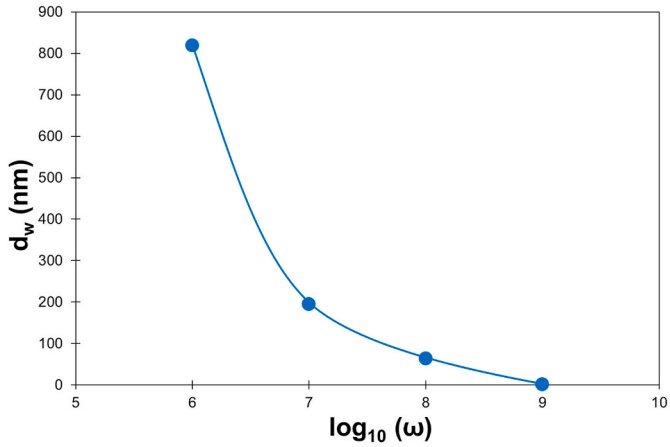

Fig. 8. Domain-wall width parameter vs angular frequency.

known.

Obtained values of μ''_S and μ''_{DW} from nonlinear fitting of experimental data show the high contribution of the domain-wall mechanism to the complex magnetic permeability - imaginary part when angular frequency is low (10^6 and 10^7 Hz). Conversely, at high angular frequencies (10^8 and 10^9 Hz) both spin rotation and domain-wall contributions are numerically small and of the same order of magnitude. The observed increase of μ''_S with angular frequency reaches a maximum at 10^7 Hz, whereas μ''_{DW} sharply decreases with the increase in angular frequency. It has also been shown that domain-wall width (d_w) decreases when angular frequency increases, yielding to a lower contribution of wall motion mechanism to the complex magnetic permeability - imaginary part.

The high values of μ''_{DW} at 10^6 and 10^7 Hz confer to the studied ferrite a high complex magnetic permeability - imaginary part, which makes it a very interesting material for EMI suppression applications at these angular frequencies.

Declaration of competing interest

The authors declare that they have no known competing financial interests or personal relationships that could have appeared to influence the work reported in this paper.

Acknowledgments

This study has been supported by Ministerio de Economía y Competitividad (Spain) through grant number (MAT2016–76320-R) and by Universitat Jaume I (Spain), grant numbers (UJIB2017-48, UJIB2020-13 and POSDOC/2020/04). Complex relative permeability determination was carried out at the central facilities (Servei Central d'Instrumentació Científica) of the Universitat Jaume I (Spain).

Appendix A. Supplementary data

Supplementary data to this article can be found online at https://doi.org/10.1016/j.ceramint.2021.07.119.

References

[1] A. Goldman, Modern Ferrite Technology, Second Editon, 2006, https://doi.org/10.1017/CBO9781107415324.004.
[2] T. Tsutaoka, Frequency dispersion of complex permeability in Mn-Zn and Ni-Zn spinel ferrites and their composite materials, J. Appl. Phys. 39 (2003) 2789–2796, https://doi.org/10.1063/1.1542651.
[3] A. Barba, C. Clausell, J.C. Jarque, L. Nuño, Magnetic complex permeability (imaginary part) dependence on the microstructure of a Cu-doped Ni–Zn-polycrystalline sintered ferrite, Ceram. Int. 46 (2020) 14558–14566, https://doi.org/10.1016/j.ceramint.2020.02.255.
[4] T. Jahanbin, M. Hashim, K. Amin Mantori, Comparative studies on the structure and electromagnetic properties of Ni-Zn ferrites prepared via co-precipitation and conventional ceramic processing routes, J. Magn. Magn Mater. 322 (2010) 2684–2689, https://doi.org/10.1016/j.jmmm.2010.04.008.
[5] C.A. Stergiou, V. Zaspalis, Analysis of the complex permeability of NiCuZn ferrites up to 1 GHz with regard to Cu content and sintering temperature, Ceram. Int. 40 (2014) 357–366, https://doi.org/10.1016/j.ceramint.2013.06.010.
[6] W.D.D. Callister, Materials Science and Engineering : an Introduction, 10th australia and new zealand edition, 2019.
[7] T. Nakamura, Study on High-Frequency Permeability in Ferrite Ceramics and Ferrite Composite Materials, Hiroshima University, 1996.
[8] T. Nakamura, Low-temperature sintering of Ni-Zn-Cu ferrite and its permeability spectra, J. Magn. Magn Mater. 168 (1997) 258–291, https://doi.org/10.1016/S0304-8853(96)00709-3.
[9] N. Ponomarenko, Study of Frequency and Microstructure Dependencies of Magnetic Losses of Ferrite Materials and Components, Riga Technical University, 2014.
[10] T. Tsutaoka, M. Ueshima, T. Tokunaga, T. Nakamura, K. Hatakeyama, Frequency dispersion and temperature variation of complex permeability of Ni-Zn ferrite composite materials, J. Appl. Phys. 78 (1995) 3983–3991, https://doi.org/10.1063/1.359919.
[11] A. Globus, Some physical considerations about the domain wall size theory of magnetization mechanisms, J. Phys. Colloq. 38 (1977), https://doi.org/10.1051/jphyscol:1977101. C1.1-C1.15.
[12] P.J. Van Der Zaag, J.J.M. Ruigrok, A. Noordermeer, M.H.W.M. Van Delden, P. T. Por, M.T. Rekveldt, D.M. Donnet, J.N. Chapman, The initial permeability of polycrystalline MnZn ferrites: the influence of domain and microstructure, J. Appl. Phys. 74 (1993) 4085–4095, https://doi.org/10.1063/1.354454.
[13] C. Guillaud, The properties of manganese-zinc ferrites and the physical processes governing them, Proc. IEE (Institution Electr. Eng. - Part B Radio Electron. Eng. 104 (1957) 165–173, https://doi.org/10.1049/pi-b-1.1957.0023.
[14] A. Globus, P. Duplex, M. Guyot, Determination of initial magnetization curve from crystallites size and effective anisotropy field, IEEE Trans. Magn. (1971) 617–622, https://doi.org/10.1109/TMAG.1971.1067200.
[15] H. Rikukawa, Relationship between mlcrostructures and magnetic properties of ferrites containing closed pores, IEEE Trans. Magn. MAG- 18 (1982) 1535–1537, https://doi.org/10.1109/TMAG.1982.1062065.
[16] M.T. Johnson, E.G. Visser, A coherent model for the complex permeability in polycrystalline ferrites, IEEE Trans. Magn. 26 (1990) 1987–1989, https://doi.org/10.1109/20.104592.
[17] J. Pankert, Influence of grain boundaries on complex permeability in MnZn ferrites, J. Magn. Magn Mater. 138 (1994) 45–51, https://doi.org/10.1016/0304-8853(94)90397-2.
[18] R.M. German, Sintering Theory and Practice, first ed., John Wiley & Sons, Inc., New York, 1996.
[19] C. Clausell, A. Barba, L. Nuño, J.C. Jarque, Effect of average grain size and sintered relative density on the imaginary part - μ″ of the complex magnetic permeability of (Cu0.12Ni0.23Zn0.65)Fe2O4 system, Ceram. Int. 42 (2016) 4256–4261, https://doi.org/10.1016/j.ceramint.2015.11.101.
[20] C. Clausell, A. Barba, L. Nuño, J.C. Jarque, Electromagnetic properties of ferrite tile absorber as a function of compaction pressure, Ceram. Int. 42 (2016) 17303–17309, https://doi.org/10.1016/j.ceramint.2016.08.026.
[21] H. Su, H. Zhang, X. Tang, Y. Jing, Z. Zhong, Complex permeability and permittivity spectra of polycrystalline Ni-Zn ferrite samples with different microstructures, J. Alloys Compd. 481 (2009) 841–844, https://doi.org/10.1016/j.jallcom.2009.03.133.
[22] L.B. Kong, Z.W. Li, G.Q. Lin, Y.B. Gan, Electrical and magnetic properties of magnesium ferrite ceramics doped with Bi2O3, Acta Mater. 55 (2007) 6561–6572, https://doi.org/10.1016/j.actamat.2007.08.011.
[23] M. Manjurul Haque, M. Huq, M.A. Hakim, Influence of CuO and sintering temperature on the microstructure and magnetic properties of Mg- Cu- Zn ferrites, J. Magn. Magn Mater. 320 (2008) 2792–2799, https://doi.org/10.1016/j.jmmm.2008.06.017.
[24] S.V. Kakatkar, S.S. Kakatkar, R.S. Patil, A.M. Sankpal, N.D. Chaudhari, P. K. Maskar, S.S. Suryawanshi, S.R. Sawant, Effect of sintering conditions and Al3+ addition on wall permeability in Ni1-xZnxAltFe2-tO4 ferrites, Mater. Chem. Phys. 46 (1996) 96–99, https://doi.org/10.1016/0254-0584(96)01746-4.
[25] A. Barba, C. Clausell, J.C.J.C. Jarque, M. Monzó, ZnO and CuO crystal precipitation in sintering Cu-doped Ni-Zn ferrites. I. Influence of dry relative density and cooling rate, J. Eur. Ceram. Soc. 31 (2011) 2119–2128, https://doi.org/10.1016/j.jeurceramsoc.2011.05.007.
[26] K.O. Low, F.R. Sale, Electromagnetic properties of gel-derived NiCuZn ferrites, J. Magn. Magn Mater. 246 (2002) 30–35, https://doi.org/10.1016/S0304-8853(01)01390-7.
[27] H.I. Hsiang, W.C. Kuo, C.S. Hsi, Sintering and cooling atmosphere effects on the microstructure, magnetic properties and DC superposition behavior of NiCuZn ferrites, J. Eur. Ceram. Soc. 37 (2017) 2123–2128, https://doi.org/10.1016/j.jeurceramsoc.2017.01.025.
[28] O.F. Caltun, L. Spinu, A. Stancu, L.D. Thung, W. Zhou, Study of the microstructure and of the permeability spectra of Ni-Zn-Cu ferrites, J. Magn. Magn Mater. (2002) 160–162, https://doi.org/10.1016/S0304-8853(01)01187-8, 242–245.
[29] T. Nakamura, T. Tsutaoka, K. Hatakeyama, Frequency dispersion of permeability in ferrite composite materials, J. Magn. Magn Mater. 138 (1994) 319–328, https://doi.org/10.1016/0304-8853(94)90054-X.
[30] W.G. Fano, S. Boggi, A.C. Razzitte, Causality study and numerical response of the magnetic permeability as a function of the frequency of ferrites using Kramers-Kronig relations, Phys. B Condens. Matter 403 (2008) 526–530, https://doi.org/10.1016/j.physb.2007.08.218.